Theoretical and Applied Fracture Mechanics 119 (2022) 103345

Contents lists available at ScienceDirect

Theoretical and Applied Fracture Mechanics

journal homepage: www.elsevier.com/locate/tafmec

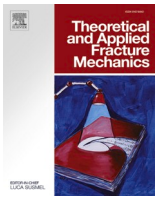

Prediction of initiation and total life in fretting fatigue considering kinked cracks

Danilo Rangel [a], Diego Erena [b,*], Jesús Vázquez [b], J.A. Araújo [a]

[a] Department of Mechanical Engineering, Faculty of Technology, University of Brasília, Campus Darcy Ribeiro, Asa Norte, Brasília, Brazil
[b] Universidad de Sevilla, Escuela Técnica Superior de Ingenieros, Departamento de Ingeniería Mecánica y Fabricación, Camino de los Descubrimientos s/n, C.P. 41092, Spain

ARTICLE INFO

Keywords:
Fretting fatigue
Fatigue crack initiation
Crack path

ABSTRACT

This work proposes a methodology to compute fretting fatigue crack initiation and total life by iterative models calibrated with fatigue stress–strain-life curves. One of the main novelty of such models is the assumption that the crack initiation length is determined by the size of the critical distance. To separate initiation and propagation lives, a numerical approach with finite elements is used. The methodology incorporates not only the multiaxial non-proportional characteristic of the stress field in fretting problems, but also the stress gradient effect. Crack initiation path is obtained by means of the SWT parameter, and to validate it, the analysed results are compared with tests considering a cylindrical-flat configuration (Aluminium 7075-T651 alloy). Most of the life initiation estimates, as well as the total life ones, are within a scatter band of 3.

1. Introduction

Fretting is a surface damage phenomenon that occurs in mechanical couplings when they are subjected to small relative displacements [1]. Some examples could be found at riveted or bolted connections, dovetail joints of turbine blades/disc fixings and overhead conductors. This surface damage often stimulates the nucleation of short crack nearby the contact surfaces edges. In presence of a bulk cyclic loading, these short cracks tend to grow and turn into failure by fretting fatigue. As many engineering assemblies are subjected to fretting, a better understanding of the phenomenon is of major interest.

Fatigue by fretting is usually divided in two phases, being them crack initiation and crack propagation. Regarding the crack initiation phase, in 1994, Cheng et al. [2] used micromechanics to model it and took dislocation pile-up under consideration. While this may be a good approach, quantitative assessment of fatigue damage at the microscopic level requires a difficult determination of physical properties. Looking for a less complex approach, Szolwinski and Farris [3] applied the Smith, Watson and Topper (SWT) multiaxial fatigue parameter [4], being able to evaluate not only fretting initiation life but the crack initiation site and direction in early propagation. In 1997 using an aluminum alloy, Lamacq et al [5] proposed a theoretical model to predict crack initiation angles and sites on fretting and later Lamacq and Dubourg [6] analyzed and correlated them to tensile and shear stress fields. Following studies, such as Neu et al. [7] and Ruiz and Chen [8] tried other parameters like the Fatemi-Socie (FS) multiaxial fatigue parameter [9] obtaining reasonable results in terms of fatigue life and crack path direction.

Further works attempt to perform models taking into account a process zone, averaging a damage parameter on a volume or critical depth [10,11]. Studies performing fatigue analysis at a single point (i.e., hot spot) was also carried. With reasonably accurate live estimations, Araujo and Nowell considered two procedures, the averaging of a critical plane fatigue parameter over a critical depth and the averaging of the stress components over a volume [11]. The critical depth and volume size were determined by best fitting experimental data. In recent developments, the Modified Wohler Curve Method (MWCM) combined with the Theory of Critical Distance (TCD) were applied to predict fatigue lives, showing a good agreement between experimental results and estimations [12,13]. The critical distance was defined in terms of stress intensity range and the endurance limit of the material and later as a function of fatigue life. In 2016, Araújo et al. averaged normal and shear stress over a line with a characteristic length and these averages were applied to critical plane criterions to examine crack initiation direction [14]. All those studies appear to have a common inconsistency, they use complete stress-life curves to calibrate their models, even though they

* Corresponding author.
E-mail address: deg@us.es (D. Erena).

https://doi.org/10.1016/j.tafmec.2022.103345
Received 27 November 2021; Received in revised form 1 April 2022; Accepted 1 April 2022
Available online 4 April 2022

are trying to estimate only the initiation life. For this reason, recent works have developed fatigue models that modify the strain-life curve by discounting the propagation phase via Linear Elastic Fracture Mechanics (LEFM) to create strain initiation-life curves. These models have been applied to predict total life in fatigue based on different multiaxial fatigue parameters as SWT and FS considering straight cracks at both phases [15-17]. Lastly the model has been applied jointly with a crack orientation method concluding that better results in terms of crack path predictions are obtained with the SWT parameter if compared with the FS parameter [18,19].

This paper proposes a methodology and two models to estimate fretting crack initiation life with an iterative model calibrated with fatigue strain-life curves, being the Model 1 with strain-life curve for total fracture of the material and Model 2 with its propagation life subtracted from strain-life curve. From a mechanical perspective, to estimate fretting initiation life with the fatigue curves corrected to initiation, as in Model 2, appears to be more reasonable. The method separates the initiation from the propagation phase considering a kinked crack at the initiation stage followed by a straight crack at the propagation stage. To do so, strain-life curves combined with a multiaxial fatigue parameter (SWT) are used to estimate crack initiation life and LEFM to estimate the propagation phase. The initiation phase is based on a critical distance method, for which the SWT parameter is averaged along a predefined length. The length of the line is defined as a function of the fatigue life by implementation of an iterative numerical method. The results are compared with cylindrical-flat contacts experimental data produced with Aluminium 7075-T651 by Martín et al.[20,21].

The estimated results in terms of crack initiation life are compared to those obtained with pseudo-experimental crack initiation results. To do so, the number of cycles to propagate the initial crack up to failure is estimated numerically and subtracted from the experimental total lives results. Besides, total life prediction is obtained and compared to the two different fatigue models.

2. Experimental campaign

In the following sections, it is described the main features of the experimental results that we used in order to check the reliability of the proposed life estimation methodology.

2.1. Fretting fatigue test set-up

To check crack initiation predictions, results are compared with an experimental fretting fatigue campaign [20,21]. In these tests, the fretting contact pair corresponds to the frequently called "cylindrical contact". In such a contact pair, a cylindrical contact pad of radius, R, is pressed against a flat surface. Fig. 1 schematically shows the device used to perform the fretting fatigue tests. With this setup, firstly the cylindrical contact pads are pressed, with a constant normal load N, against the flat surface of a dog-bone type fretting fatigue test specimen. Then, a fully reversed (R = -1) cyclic axial load with amplitude, P, is applied to the fretting fatigue test specimen by means of a hydraulic actuator. This cyclic axial load produced an in phase tangential load with amplitude, Q, at the contact pads. A very interesting characteristic of the present device is, that for a certain value of P, the tangential load amplitude can be modified independently of the axial load amplitude, merely moving the adjustable supports (see Fig. 1**a**).

Both contact pads and test specimens were made in aluminium alloy Al 7075-T651, which is widely used in the manufacture of aircraft components: wing skins, panels, covers, seat rear legs, and seat spreader [22,23]. The chemical composition and main mechanical and fatigue properties for this material are shown in Table 1 and Table 2.

The crack profiles of a pair of test carried in the same test campaign as those shown in the current paper are depicted in Refs. [18,19,24]. The observed cracks tend to the vertical direction (perpendicular to the contact surface) in this type of fretting configuration. The slope of the initial crack, from the surface up to a length of approximately 150 μm, is

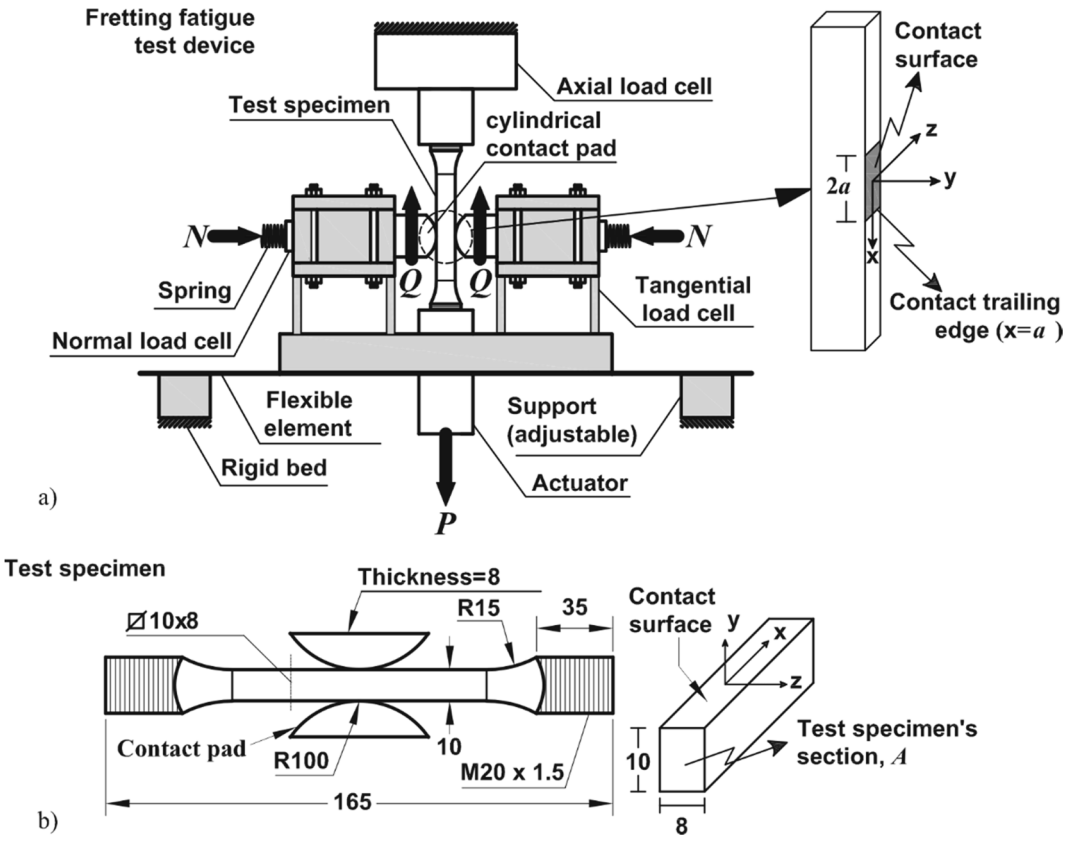

Fig. 1. a) Scheme of the fretting fatigue test set up. b) main geometric characteristic of the fretting fatigue specimen (mm).

Table 1
Chemical composition (% weight) for the Al 7075-T651.

Chemical composition (% weight) [24,25]										
%	Al	Zn	Mg	Cu	Fe	Si	Mn	Cr	Ti	Others
Max	91.4	6.1	2.9	2.0	0.5	0.4	0.3	0.28	0.2	0.05
Min	87.1	5.1	2.1	1.2	–	–	–	0.18	–	–

Table 2
Main mechanical and fatigue properties for the Al 7075-T651.

Mechanical and fatigue properties					
Young's modulus [25]	E	$70{\cdot}10^3$ MPa	Ramberg-Osgood cyclic hardening coefficient [26]	K'	712 MPa
Poisson's ratio [25]	ν	0.33	Ramberg-Osgood cyclic hardening exponent [26]	n'	0.041
Yield strength*	σ_y	503 MPa	fatigue strength coefficient [26]	σ_f'	995 MPa
Tensile strength*	σ_u	572 MPa	fatigue ductility coefficient [26]	ε_f'	0.0994
Mode I SIF threshold (R = 0.1) [27]	ΔK_{th}	2.2 MPa$\sqrt{m}$	fatigue strength exponent [26]	b	−0.09413
Pari's law coeff. (R = 0, m/cyc. and MPa$\sqrt{m}$) [28]	C	$8.831{\cdot}10^{-11}$	fatigue ductility exponent [26]	c	−0.5778
Pari's law exp. (R = 0) [28]	m	3.322	Grain size*	d	50 μm
Fatigue limit [29]	$\Delta\sigma_{-1}$	169 MPa	Fracture toughness [30]	K_{Ic}	43.9 MPa$\sqrt{m}$

* Data obtained in our laboratory.

below 20°.

2.2. Test results

In Table 3 it is shown the fretting fatigue lives experimentally obtained with the corresponding fretting loads. In addition, and in order to compare the fretting conditions among different tests, its corresponding Hertzian theoretical parameters –assuming plane strain conditions- are also shown in the above table. In that table, a_H is the contact semi-width and $\Delta\sigma_{xx}$ is the range of the direct stress at the contact trailing edge, $x = a_H$ (see Fig. 1**a**). These two parameters are defined by the following equations [31]:

$$a_H = \sqrt{\frac{8N^*R(1-\nu^2)}{\pi E}} \tag{1}$$

$$\Delta\sigma_{xx} = \sigma + 4\mu p_0 \frac{c_H}{a_H}\sqrt{\left(\frac{a_H+e}{c_H}\right)^2 - 1} \tag{2}$$

In the above equations, $N^* = N/t$ (being t the test specimen thickness), $\sigma = P/A$ is the amplitude of the test specimen bulk (axial) stress,$\boldsymbol{P}$ is the amplitude of the bulk load (see Fig. 1**a**), A is the test specimen net section, p_0 is the maximum surface normal pressure, $\boldsymbol{c_H}$ is the contact stick zone half-width, e is the eccentricity of the stick zone, and μ is the coefficient of friction being this parameter equal to 0.75 according to [20]**.** Expressions for the above parameters are [31]:

$$p_0 = \frac{2N^*}{\pi a_H} \tag{3}$$

$$c = a_H\sqrt{1 - \frac{Q}{\mu N}} \tag{4}$$

$$e = \frac{R\sigma(1-\nu^2)}{\mu E} \tag{5}$$

2.3. Material fatigue curve

A key factor for crack initiation predictions is the uniaxial fatigue data. In fretting fatigue, high stresses values are produced at the contact zones, and thus fatigue data for low-cycle fatigue regime are often required. In this work we have used the constant strain amplitude fatigue data (ε-N curve) provided by the Japanese National Institute for

Table 3
Fretting fatigue lives, loads, thickness, and related Hertzian parameters for analysed tests.

Test type	N(N)	Q(N)	σ(MPa)	N_f(Cycles)		t(mm)	a_H(mm)	c(mm)	p_0(MPa)	e (mm)	$\Delta\sigma_{xx}$ (MPa)
1	6629	971	70	316,603	165,696	8	1.64	1.47	321.87	0.12	637.61
2	5429	971	110	112,165	126,496	8	1.48	1.29	291.28	0.19	731.64
3	5429	1257	110	120,663	113,799	8	1.48	1.23	291.28	0.19	773.38
4	4217	1543	110	88,216	89,376	8	1.31	0.94	256.72	0.19	796.22
5	5429	1543	110	87,481	82,559	8	1.48	1.17	291.28	0.19	812.65
6	3006	971	150	60,040	59,234	8	1.10	0.83	216.74	0.25	782.19
7	4217	971	150	67,776	60,288	8	1.31	1.09	256.72	0.25	810.03
8	5429	971	150	47,737	51,574	8	1.48	1.29	291.28	0.25	833.19
9	3006	1543	150	19,223	39,408	8	1.10	0.62	216.74	0.25	861.99
10	4217	1543	150	50,369	39,001	8	1.31	0.94	256.72	0.25	886.83
11	5429	1543	150	50,268	39,202	8	1.48	1.17	291.28	0.25	907.64
12	3006	2113	150	34,904	41,002	8	1.10	0.28	216.74	0.25	933.47
13	4217	2113	150	34,716	40,004	8	1.31	0.75	256.72	0.25	956.11
14	5429	2113	150	32,339	36,431	8	1.48	1.03	291.28	0.25	975.18
15	3006	971	175	26,587	31,815	8	1.10	0.83	216.74	0.30	838.55
16	4217	971	175	27,724	32,843	8	1.31	1.09	256.72	0.30	869.46
17	5429	971	175	35,171	29,100	8	1.48	1.29	291.28	0.30	895.12
18	3006	1543	175	31,224	30,154	8	1.10	0.62	216.74	0.30	914.98
19	4217	1543	175	34,748	34,930	8	1.31	0.94	256.72	0.30	942.82
20	5429	1543	175	33,349	28,005	8	1.48	1.17	291.28	0.30	966.10
21	3006	2113	175	21,669	21,207	8	1.10	0.28	216.74	0.30	983.99
22	4217	2113	175	26,989	28,595	8	1.31	0.75	256.72	0.30	1009.53
23	5429	2113	175	28,112	28,178	8	1.48	1.03	291.28	0.30	1031.00

Materials Science (NIMS)[26]. Previously, in Table 2 we have shown the ε-N curve parameters obtained by linear regression, on a log–log scale, for the elastic and plastic strain amplitude, ($\sigma_f^{'}$, b) and ($\varepsilon_f^{'}$, c) respectively. Here to complete this information, we want to show these fatigue data in addition to the regression fitting curve. These data are shown in Fig. 2, in which it can be readily observed the wide range in fatigue lives for this set of experimental fatigue results (from about 10^2 up to 10^8 cycles) and thus covering from the low-cycle to very high-cycle fatigue regime. In addition, one can see for many strain amplitude levels that more than two test have been performed. Thus, this set of data provide us with a good confidence on the fatigue response for this aluminium alloy.

3. Crack initiation life prediction. Based on ε-N curve

As a first attempt, crack initiation and total life will be obtained based on the fatigue curve of the material in the form SWT-N_T (where N_T are number of loading cycles to complete fracture of the specimens) and the LEFM procedures. The estimations use an analytical solution to obtain the contact stress field, as described in more details by Hills and Nowell [1], and later such a stress field is applied to a critical plane multiaxial fatigue model. The stresses, the crack orientation, the crack initiation length and the initiation life are determined by an interactive computational process. With that, the propagation life is estimated by a numerical model computed with Abaqus software by means of the Extended Finite Element Method (XFEM) as there is no analytical solution for kinked cracks as those observed in fretting fatigue problems.

3.1. Procedure to estimate crack initiation

As the cracking process has a directional nature, the use of a critical plane approach is widely recognized as appropriate with a variety of studies showing its capability to predict the fatigue strength of metallic materials and its life [32-42].

3.1.1. The critical direction method.

Following Araujo et al. [14] critical plane approaches have been developed based on the cracking behavior under uniform stress/strain conditions. Under such type of stress fields, the classical method to determine the crack initiation orientation and life is to search for the critical plane in a single material point. Unfortunately, for mechanical problems under high stress gradients, such as the cylinder-flat contact problem under partial slip regime, the material point at which the critical plane should be computed is not evident because of this range of different stress states within small zones under the contact surface.

Therefore, in this work, the critical direction method was considered to compute the critical plane under fretting conditions. This method associates the critical plane with a physical dimension, differing to the point concept. When applied to a bidimensional case, as the cylindrical-flat fretting contact, this plane turns in to a line and each line indicates the possible crack initiation direction. The stress influence is considered taking the average stresses along the line.

To implement the method above, a line with a characteristic length of $2L$ (determined subsequently) and an orientation θ starting at the crack initiation point is taken as shown in Fig. 3. Hence, the average of the normal stresses along the line is given by **Eq. (6)**.

$$\overline{\sigma}_n(\theta,t)=\frac{1}{2L}\int_0^{2L}\sigma_n(r,\theta,t)dr \tag{6}$$

where $\sigma_n(r,\theta,t)$ is the normal stress component to the inclined line at each time instant, t.

Also, the average values of the maximum normal stress and of the normal stress amplitude, with respect to the line, are determined by **Eq.**

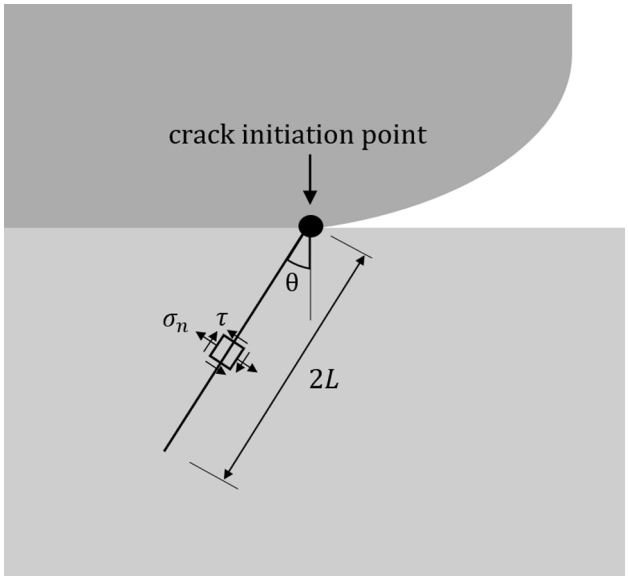

Fig. 3. Schematic representation of the critical direction method at the trailing edge of the contact. The angle θ is positive in the clockwise direction.

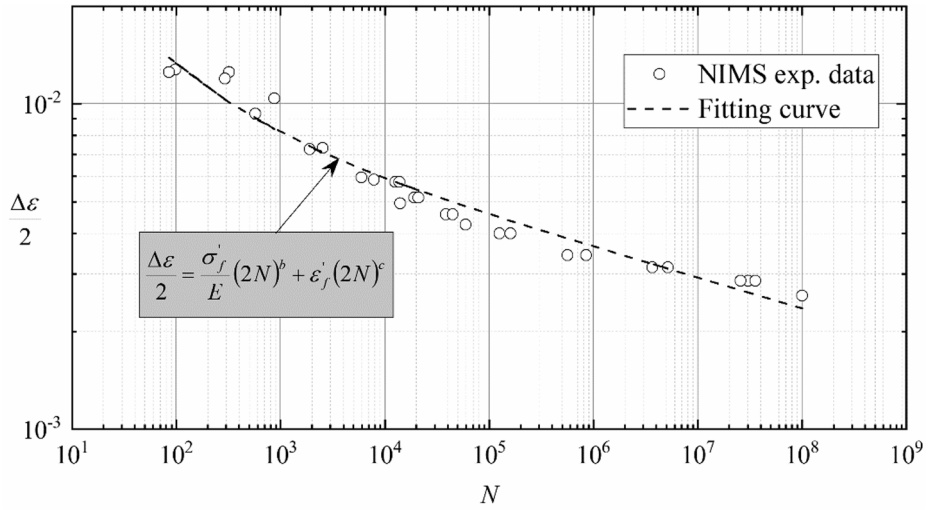

Fig. 2. Experimental and fitting curve (ε-N curve) for the NIMS constant strain amplitude fatigue data.

(7) and **Eq. (8)**.

$$\overline{\sigma}_{n,max}(\theta) = \max|_t \overline{\sigma}_n(\theta, t) \tag{7}$$

$$\overline{\sigma}_{n,a}(\theta) = \frac{1}{2}\left(\max|_t \overline{\sigma}_n(\theta, t) - \min|_t \overline{\sigma}_n(\theta, t)\right) \tag{8}$$

3.1.2. Smith-Watson-Topper parameter and initiation life estimation.

After evaluating the average stresses as above, the chosen fatigue damage parameter was the Smith-Watson-Topper (SWT) [4]. Originally created to consider the mean stress effect under uniaxial loading, Socie [32] proposed to extend the SWT parameter use to materials and loading conditions where the cracking phenomenon is normal stress/strain dominated. The SWT parameter, in the stress-based form, can be expressed as.

$$SWT = \max\left\{\sqrt{\sigma_{n,a}(\theta)\sigma_{n,max}(\theta)}\right\} \tag{9}$$

where the $\sigma_{n,a}$ is the normal stress amplitude and $\sigma_{n,max}$ is the maximum normal stress in the loading cycle for each θ orientation. According to Chu [43], the correct procedure to determine the critical plane is to define it as the material plane where the fatigue parameter, **Eq. (9)**, is maximum. Note, that for the critical distance method, the stresses will be the average across the line.

3.1.3. Crack initiation size and determination of variable length L.

There is no consensus in the academic community about the crack length scale which separates the initiation from the propagation life phases. Hence, in this study, we assume the crack initiation size will coincide with the length of the material critical distance, which depends on life [13]. The life dependent critical distance can be determined by fitting a line *L-N* in the logarithmical scale (log–log), as depicts Fig. 4, where the static characteristic length L_s and the infinite life characteristic length L_∞ are respectively **Eq. (10)** and **Eq. (11)**,

$$L_s = \frac{1}{\pi}\left(\frac{K_{Ic}}{\sigma_u}\right)^2 \tag{10}$$

$$L_\infty = \frac{1}{\pi}\left(\frac{\Delta K_{th}}{\Delta\sigma_{-1}}\right)^2 \tag{11}$$

K_{Ic} is the material mode I fracture toughness, σ_u is the ultimate tensile strength, ΔK_{th} is the threshold stress intensity factor range for fully reversed mode I loading and $\Delta\sigma_{-1}$ is the uniaxial fatigue limit range for a loading ratio $R = -1$, determined at so called infinite fatigue life, N_∞.

This procedure returns constants A and B equal to 1.875 mm and −0.3752, respectively. Therefore, the equation linear log–log equation turns into **Eq. (12)**, with L in millimeters.

$$L = 1.875(N_i)^{-0.3572} \tag{12}$$

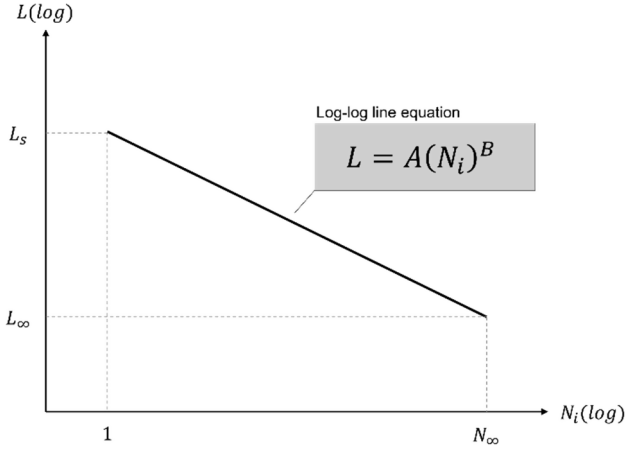

Fig. 4. Log-log fitting for the critical distance *L*.

3.1.4. Initiation life estimation

As previously mentioned, the initiation life estimation is conducted by using the constant strain amplitude fatigue data provided by the Japanese National Institute of Materials Science (NIMS) that leads to the following SWT-life equation.

$$SWT = \frac{\sigma_f'^2}{E}(2N_t)^{2b} + \sigma_f'\varepsilon_f'(2N_t)^{b+c} \tag{13}$$

where, as in Table 2, σ_f' and b are the fatigue strength coefficient and exponent, respectively, ε_f' and c the fatigue ductility coefficient and exponent, respectively, E is the Young's modulus and N_t is the life to complete separation of the specimen.

It should be noted that in a fatigue situation having a stress gradient, like fretting, it is quiet frequent the use of **Eq. (13)** to predict the crack initiation cycles, merely assuming that $N_t = N_i$ and computing the fatigue parameter at a certain length from the surface [3,15,16,44]. Then the value of N_i, for a certain value of the SWT parameter, is obtained numerically solving **Eq. (13)**.

3.1.5. Iterative calculation algorithm

With all mentioned calculations, it is possible to compute the crack initiation length and inclination, the SWT parameter and the estimated life. As we have a system of equations, a numerical iterative approach is required to determine such values. They are computed using iterations and adapting the numerical bisection method [45], as explained next.

The flowchart depicted in Fig. 5 illustrates the steps of this process. Such a process starts by the guess of a length, L_G. In the initial step, the possible range for the crack initiation length is $[L_{min}, L_{max}]$, where $L_{min} = L(N = 1)$ and $L_{max} = L(N_\infty = 10^6)$. This guessed value is the midpoint between the range, $L_G = \frac{L_{max}+L_{min}}{2}$. The relevant average stresses are then calculated over all material planes with inclination θ and length $2L_G$. The critical plane is determined by the angle θ which maximizes the multiaxial fatigue parameter, hence, returning the SWT_G. This provides all the conditions to determine, by means of **Eq. (12)**, the initiation life N_G associated to this critical length L_G. With SWT_G and N_G, a new crack initiation length, L_i, is determined for comparison, using the **Eq. (13)**. In case L_i is greater than L_G, for the next iteration, $L_{min} = L_G$, altering the possible range. And if L_i is less than L_G then, $L_{max} = L_G$, and so, the method restarts. Thus, one should notice that, after each iteration, the possible range is halved, similar to the bisection method, until $L_i = L_G$ within an acceptable tolerance, when the process ends.

3.2. XFEM model and crack propagation calculations

The aforementioned test configuration is modelled in Abaqus software by means of the extended finite element method (XFEM) for crack modelling on a single mesh. More details and information about the XFEM formulation could be found in references [46-48]. Due to the nature of the contact pair and the relation between the contact width and the total thickness of the specimen, plane strain conditions are assumed with a reasonable confidence according to former work [49]. Only a contact pair is modelled due to symmetry conditions of the set up. To reproduce the actual test performance, loads are applied in three steps (see Fig. 6**a**). First the normal load is applied, N^*, and it remains constant. The second step applies the bulk stress, σ, and the shear force, $Q^* = Q/t$, in phase but in opposite directions. Finally, the last step applies the same values of σ and Q^*, but both in the opposite direction of the previous step. Global dimensions, main parameters and boundary conditions of the model are shown in Fig. 6**b**. Loads Q^* and N^* are applied to a master node that transfer the loads to all nodes lying on the top of the punch (see Fig. 7). The rotational movement of the master

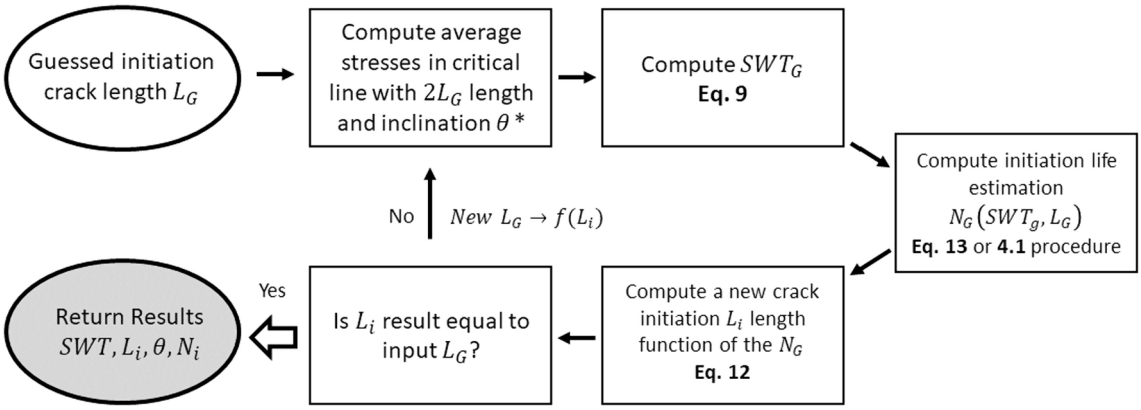

Fig. 5. Flowchart of interactive algorithm for initiation life computation.

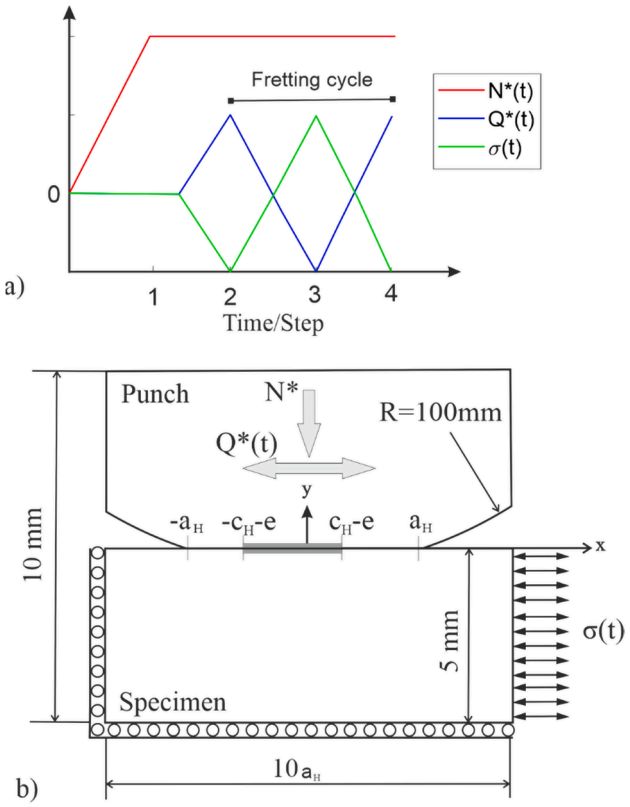

Fig. 6. a) Scheme of the load sequence; b) Main model parameters.

node is restricted.

Quadrilateral elements are used to mesh the parts, considering a bilinear formulation and plane strain conditions. The contact pair is defined using the master–slave algorithm for contact between two surfaces. Lagrange multiplier formulation is considered in the contact pair to define the frictional behaviour of the parts assembled and assuming a constant-non-varying with fretting cycles- coefficient of friction $\mu = 0.75$. Contact of the crack faces in the XFEM model are considered as frictionless. In view of the contact stresses showed in Table 3, and the yield stress for the Al 7075-T765, the material behaviour in the model is considered linear elastic.

The mesh size of the model is 5 μm × 5 μm around the trailing edge and propagates up to the end of the specimen (see Fig. 7). Thus, it is possible to capture the stepped stress/strain gradients appearing at the crack tip and to obtain more accurately the stress intensity factors (SIFs) of cracks introduced.

The XFEM technique allows the simulation of cracks, which are introduced after the meshing process. The estimated crack initiation lengths are introduced in the model with its corresponding orientation (see Fig. 7). The initial crack is propagated incrementally considering that its orientation is straight and perpendicular to the contact surface. For each crack increment the model is solved to compute its corresponding SIFs ahead the crack tip. Mode I and II SIFs are computed via the interaction integral method implemented in Abaqus for loading steps 2 and 3, and thus enabling to compute the SIFs range in a fretting cycle. The crack propagation increment considered is $\Delta a = 100\mu m$ (Represented by blue points in Fig. 7). Once the SIFs are known for each crack length it is possible to estimate the crack propagation lifetime integrating the fatigue crack growth law. In order to take into account both SIFs modes, an equivalent ΔK_{eq} is obtained using the expression proposed by Tanaka et al. [50] and integrating the Paris crack growth law.

$$\Delta K_{eq} = \sqrt[4]{\Delta K_I^4 + 8\Delta K_{II}^4} \tag{14}$$

$$\frac{da}{dN_p} = C(\Delta K)^m \tag{15}$$

3.3. Results model 1

The results obtained applying the described procedures for crack initiation and propagation are shown in Table 4 for each specific test configuration. The third column of such table contains the average values of the SWT parameter obtained along the critical plane whose length and inclination are also reported. The number of cycles to initiate a crack, N_i, of length, $2L$, is obtained from **Eq. (13)** and the SWT parameter obtained for each test, assuming that $N_t = Ni$ in **Eq. (13).** The number of cycles to propagate the former cracks from $2L$ up to final fracture, that in this case is considered when the cracks reach the border of model, is obtained according to the procedure described in **3.2.** The border of the model defines the maximum crack length which is 5 mm, for this value the SIF is near the K_{Ic} value and then the crack growth rate is high. Therefore, the error made when setting the crack length equal to 5 mm, if compared with the propagation up to a length causing $K = K_{Ic}$, is negligible. The sum of both, initiation and propagation cycles is the estimated total life, N_T. Besides, in order to compare the initiation estimated cycles, a pseudo-experimental value of initiation cycles, N_i^{exp} is computed by subtracting from the experimental number of total cycles, N_f, from Table 3, the propagation life numerically obtained, N_p. Worth noting that, in some cases, the number of cycles to propagate a crack is larger than the experimental total life. For these cases a negative N_i^{exp} is obtained, which is a non-sense, thus we assume in these situations that $N_i^{exp} = 1$.

To ease the comparison to the reader the results in Table 4 are depicted in Fig. 8. The results in term of initiation life are shown in

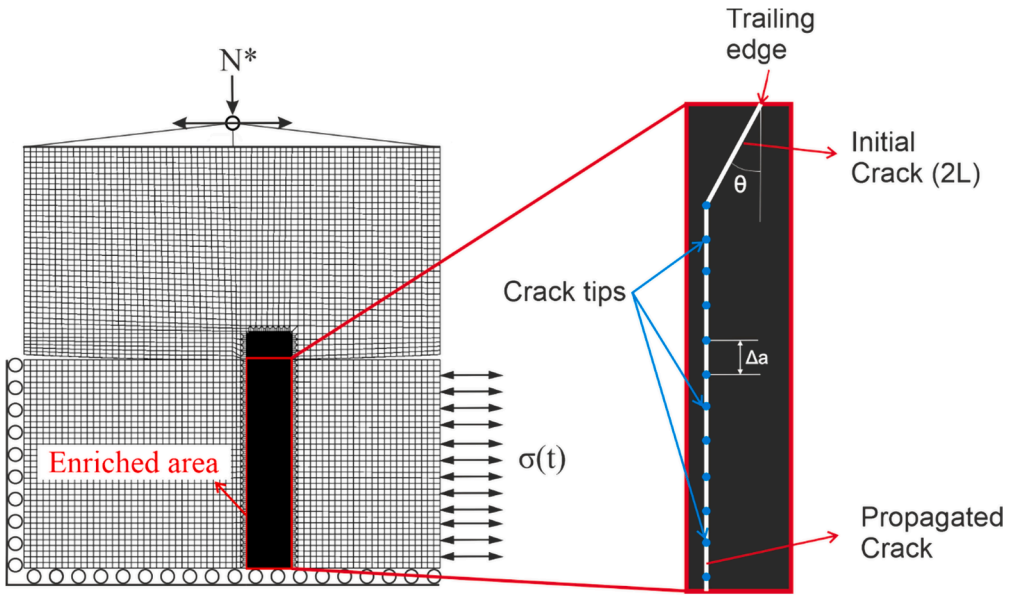

Fig. 7. Mesh and boundary conditions.

Table 4
Fretting results obtained by means of model 1.

Test type	2L (μm)	θ°	SWT	N_i (Cycles)	$N_i^{exp} = N_f - N_p$ (Cycles)		N_p (Cycles)	N_T (Cycles)
1	17	5	0.99	317,079	1	1	452,075	769,154
2	25	5	1.30	85,275	58,195	1	53,970	139,245
3	30	5	1.44	51,967	79,332	20,501	41,331	93,298
4	33	5	1.56	36,179	64,964	29,945	23,252	59,431
5	34	5	1.59	33,390	54,804	16,492	32,677	66,067
6	33	5	1.55	37,768	43,620	5046	16,420	54,188
7	35	5	1.61	31,458	48,110	9164	19,666	51,124
8	36	5	1.66	27,160	1081	1	46,656	73,816
9	43	5	1.86	16,057	7722	11,850	11,501	27,558
10	44	5	1.91	14,236	36,818	11,214	13,551	27,787
11	45	5	1.95	12,926	18,414	1	31,854	44,780
12	52	5	2.17	8108	25,897	23,887	9007	17,115
13	54	5	2.21	7532	24,470	22,226	10,246	17,778
14	55	5	2.24	7057	9403	6438	22,936	29,993
15	39	5	1.76	20,550	14,863	1	11,724	32,274
16	42	5	1.84	17,062	15,813	3870	11,911	28,973
17	44	5	1.90	14,704	22,949	2174	12,222	26,926
18	50	5	2.09	9663	22,579	11,846	8645	18,308
19	52	5	2.15	8526	25,788	17,444	8960	17,486
20	53	5	2.20	7677	24,016	10,995	9333	17,010
21	60	5	2.40	5239	15,068	9367	6601	11,840
22	61	5	2.45	4818	20,137	16,925	6852	11,670
23	63	5	2.49	4486	20,776	16,356	7336	11,822

Fig. 8**a,** where the pseudo-experimental initiation lives are represented against the predicted values. Note that cases with $N_i^{exp} = 1$ does not appear in the figure. Taking into account the complex definition of crack initiation length and number of cycles to initiate a crack, the results are quite reasonable and the great majority of them lie within a scatter band of 2 and 3. As far as total life (initiation plus propagation lives) prediction, Fig. 8**b** depicts that the results are even more satisfactory, noticing that almost all the points are inside a scatter band of 2. Only the results of the type test 1 are a bit far from the scatter band. However, this is not remarkable since the own dispersion of the two tests shown is high.

4. Crack initiation life prediction. Based on ε*-N_i curves

4.1. Computation of ε*-N_i curve

In former sections, the initiation life was estimated based on the SWT-N_t curve (see **Eq.** (13)). However, it is important to note that this curve represents the cycles up to final fracture of the strain controlled test specimen, which means that initiation and propagation cycles are joined in the life term. Nevertheless, from a mechanical standpoint and due to the iterative model proposed in the current work, it makes more sense to consider the curve of the fatigue parameter versus the number of cycles for crack initiations (SWT-N_i). These curves could be obtained based on **Eq.** (16) and represents the number of cycles (N_i) required to nucleate a specific crack length (2L) for each SWT level. To create these curves, it is necessary to know the conditions, both geometrical and load, under which the tests were carried out in order to obtain the curve shown in Fig. 2. The generated curves should be understood as a material property.

To do so **Eq.16** is applied for all possible SWT values and initiation lengths, 2L. Which means that for each initiation length a new curve is generated.

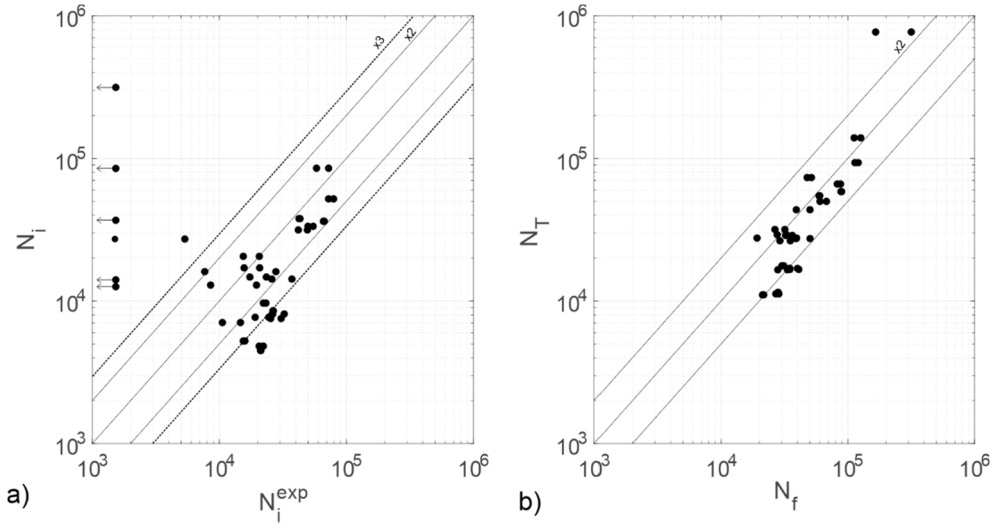

Fig. 8. a) Comparison of the pseudo-experimental initiation lives against the predicted values, b) Comparison of experimental estimated total number of cycles to complete fracture.

$$N_i(SWT, 2L_i) = N_T(SWT) - N_p(SWT, 2L_i) \quad (16)$$

In **Eq. (16)** N_i is the number of cycles to initiate/nucleate the crack $2L$, N_T is the total number of cycles obtained from **Eq. (13)**, N_p is the number of cycles to propagate the crack $2L$ up to failure integrating the Pariś crack growth law.

The fatigue curve of the material used in the current work is the one defined by **Eq.13** and the material parameters of Table 2**.** The constant strain amplitude fatigue curve was obtained with cylindrical specimens with a diameter of 7 mm and stress ratio R = -1 via uniaxial tests [26]. Subtracting the value of σ_{max} from **Eq. (9)** it is possible to compute $\Delta K_I(a) = \sigma_{max} Y \sqrt{\pi a}$. Where the corrective factor Y, is obtained from Nasgro software, considering a semi-elliptical crack growing in a cylindrical specimen and a ranging from $2L$ up to $a_f = 5$ mm.

Integrating the ΔK_I and applying **Eq.16** it is possible to generate the so called initiation curves for which an example is depicted in Fig. 9**.** It is important to note that, there is a stress level depending on the initial crack length considered, above which the propagation cycles,N_p, are higher than the estimated total cycles,N_T, obtained from **Eq.13.** In these cases, the initiation cycles computed according to **Eq.16** are negative, which is a physically meaningless. Therefore, a value of one cycle is assigned to the initiation phase in these stress levels.

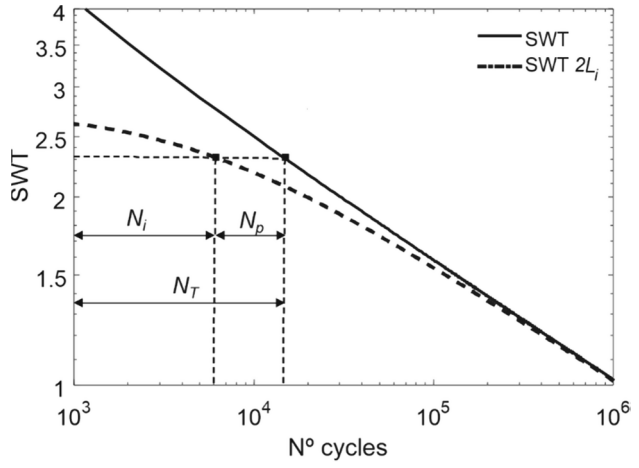

Fig. 9. Creation of initiation curves *SWT-N_i* with propagation lives computed by the Pariś law.

4.2. New procedure to estimate crack initiation

For the computation of the fretting fatigue initiation life with ε*-N_i, which discards the propagation cycles, the procedure as adopted follows the same steps as those described in Section **3.1**, except that presented in Section **3.1.4.**

Therefore, for the initiation life estimative, instead of using the **Eq. (13)** with NIMS constants, it uses the initiation curves according to **Eq. (16)**, which could be called as *SWT-N_i* curves. Here it should be stressed again that, in such curves, the number of cycles to propagate the crack (from a specific crack length, $2L$, up to final fracture) was subtracted from those provided by NIMS equation as explained in Section **4.1**. This way, the computation with the incremental analysis utilizes these curves to determine *SWT*, θ, $2L$ and the Initiation life N_i.

4.3. Results model 2

The results considering the new procedure are reported in Table 5**.** Besides, in Fig. 10 the results are plotted together with those obtained by the use of model 1 for comparative purposes. As was already the case with model 1, the results in terms of initiation life have a very large dispersion. Even more so in model 2 than in model 1. However, these results are only shown for illustrative purposes.

In order to quantify which method predicts best results, the data is adjusted with a regression line to a curve of the type $N_T = N_f$. In the case of model 1 the squared correlation factor is $R^2 = 0.67$, on the other hand the same parameter for model 2 is 0.57. Therefore, quantitatively model 1 results in slightly better total life predictions.

5. Discussion and conclusions

A new fretting fatigue model has been proposed and validated. The main novelty of such model is that it assumes that the crack initiation length is determined by the size of the critical process fatigue zone. The methodology proved capable to incorporate not only the multiaxial non-proportional characteristic of the loading history but also the stress gradient always present in mechanical couplings under fretting conditions. The orientation of the initial crack is obtained by means of the multiaxial SWT parameter. The later propagation phase of the crack is considered to be straight and perpendicular to the surface. From this point, lives were estimated by two different models. In Model 1 the estimated initiation life for a $2L$ crack is computed by an iterative process but considering a strain-life curve for total fracture of the material.

Table 5
Fretting results obtained by means of model 2.

Test	2L (μm)	θ°	SWT	N_i (Cycles)	N_i ^{exp} = N_f-N_p (Cycles)		N_p (Cycles)	N_T (Cycles)
1	15	5	1.02	504,796	1	1	452,075	956,871
2	23	5	1.32	112,142	58,195	1	53,970	166,112
3	28	5	1.46	61,007	79,332	11,461	41,331	102,338
4	32	5	1.57	38,881	65,915	28,194	22,301	61,182
5	33	5	1.59	35,073	54,781	14,786	32,700	67,773
6	32	5	1.56	41,132	43,158	1220	16,882	58,014
7	34	5	1.61	32,406	49,323	9429	18,453	50,859
8	36	5	1.66	26,672	1507	1	46,230	72,902
9	45	5	1.84	13,082	7669	14,772	11,554	24,636
10	47	5	1.89	11,181	37,236	14,687	13,133	24,314
11	49	5	1.92	9832	19,603	1	30,665	40,497
12	63	5	2.10	4487	26,357	27,968	8547	13,034
13	65	5	2.13	3996	25,353	26,645	9363	13,359
14	67	5	2.15	3651	10,569	11,010	21,770	25,421
15	41	5	1.76	18,310	15,423	2341	11,164	29,474
16	44	5	1.82	14,294	15,663	6488	12,061	26,355
17	47	5	1.87	11,705	23,453	5677	11,718	23,423
18	57	5	2.04	6036	23,259	16,153	7965	14,001
19	61	5	2.08	4950	26,416	21,648	8332	13,282
20	64	5	2.12	4218	24,487	14,925	8862	13,080
21	80	5	2.28	2015	15,881	13,404	5788	7803
22	83	5	2.30	1798	20,583	20,391	6406	8204
23	85	5	2.33	1635	21,122	19,553	6990	8625

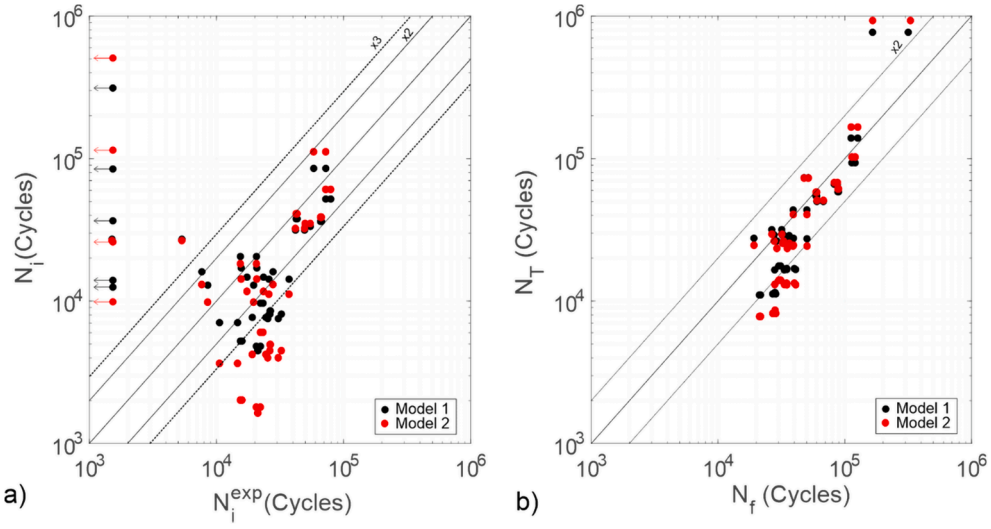

Fig. 10. a) Comparison of the pseudo-experimental initiation lives against the predicted values by Models 1 and 2, b) Comparison of experimental versus estimated total number of cycles to complete failure (Models 1 and 2).

In Model 2 the material strain-life curve was corrected subtracting from it the number of cycles to propagate the crack. Since crack initiation length, 2*L*, was considered to be variable in function of life, it means that, there will be many strain-life curves each being for a specific crack initiation length. From a mechanical point of view, Model 2 seems to be more coherent since it estimates fretting initiation life from a basic plain fatigue strain-life curve where the propagation stage was already discounted.

The strongest hypothesis assumed in this work is concerned with the size of material process zone being the crack initiation length. However, this should be considered quite reasonable since the critical process zone is assumed to vary with life. Here, such life is the necessary number of cycles for the crack to be contained within such process zone.

Comparisons for this limited range of tests with cylinder on flat geometries of Al 7075-T651 alloy under partial slip regime allowed us to conclude that the initiation lives estimated by Model 1 were more accurate than those estimated by Model 2. Also, the results improved for both models when total estimated life (estimated initiation plus propagation) is compared to the experimental fretting life for complete fracture.

The fact that Model 1 provided better results than Model 2 apparently seems as a lack of consistency from a mechanical viewpoint. This may be related to the simplified manner that the L-N curve was obtained in this work. One should notice that the most precise way to extract such a curve is by means of an experimental fatigue campaign which provides S-N curves for plain and for sharply notched specimens. Ideally, these specimens should be manufactured from the same aluminium batch used to obtain the fretting specimens. Future additional work with more refined ways to obtain the fatigue material constants should be conducted to draw more firm and wide conclusions.

Declaration of Competing Interest

The authors declare that they have no known competing financial interests or personal relationships that could have appeared to influence the work reported in this paper.

Acknowledgments

The authors would like to acknowledge the financial support of Transmissoras Brasileiras de Energia (TBE) for the project entitled Fadiga de Cabos de Alumínio Liga (CAL) 1120 e 6201: Estudo Comparativo, Efeito de Grampos AGS e de Emendas Pré-formadas. This project has been funded in the context of the Research and Development Program of the Brazilian National Agency of Electric Energy (ANEEL). The authors would also like to thank CAPES – Finance Code 001 (Coordenação de Aperfeiçoamento de Pessoal de Nível Superior) and CNPq – Finance Code 001 (Conselho Nacional de Desenvolvimento Científico e Tecnológico) for the research grant. These supports are gratefully acknowledged.

References

[1] D.A. Hills, D. Nowell, Mechanics of fretting fatigue, Kluwer Academic Publishers, Dordrecht, Boston, 1994.
[2] W. Cheng, H.S. Cheng, T. Mura, L.M. Keer, Micromechanics modeling of crack initiation under contact fatigue, ASME Trans. 116 (1994) 2–8.
[3] M.P. Szolwinski, T.N. Farris, Mechanics of fretting fatigue crack formation, Wear 198 (1-2) (1996) 93–107.
[4] R.N. Smith, P. Watson, A. Topper, Stress-strain function for the fatigue of metals, J. Mater. JMSLA 5 (1970) 767–778.
[5] V. Lamacq, M.-C. Dubourg, L. Vincent, A theoretical model for the prediction of initial growth angles and sites of fretting fatigue cracks, Tribol. Int. 30 (6) (1997) 391–400.
[6] V. Lamacq, M. Dubourg, Modeling of initial fatigue crack growth and crack branching under fretting conditions, Fatigue Fract. Eng. Mater. Struct. 22 (1999) 535–542.
[7] R.W. Neu, J.A. Pape, D.R. Swalla-Michaud, Methodologies for linking nucleation and propagation approaches for predicting life under fretting fatigue, in: D. W. Hoeppner, V. Chandrasekaran, C.B. Elliot (Eds.), Fretting fatigue: current technology and practices, ASTM STP 1367, ASTM, West Conshohocken (PA), 1999.
[8] C. Ruiz, K.C. Chen, Life assessment of dovetail joints between blades and discs in aero-engines. In: Proc Int Conf on Fatigue Sheffield: I Mech E; 1986.
[9] A. Fatemi, D.F. Socie, A critical plane approach to multiaxial fatigue damage including outof-phase loading, Fatigue Fract. Eng. Mater. Struct. 11 (3) (1988) 149–165.
[10] D. Nowell, D. Dini, D.A. Hills, Recent developments in the understanding of fretting fatigue, Eng. Fract. Mech. 73 (2) (2006) 207–222.
[11] J. Araújo, D. Nowell, The effect of rapidly varying contact stress fields on fretting fatigue, Int. J. Fatigue 24 (2002) 763–775.
[12] J. Araujo, L. Susmel, D. Taylor, J. Ferro, E. Mamiya, On the use of the theory of critical distances and the Modified Wöhler curve method to estimate fretting fatigue strength of cylindrical contacts, Int. J. Fatigue 29 (1) (2007) 95–107.
[13] J.A. Araújo, L. Susmel, M.S.T. Pires, F.C. Castro, A multiaxial stress-based critical distance methodology to estimate fretting fatigue life, Tribol. Int. 108 (2017) 2–6.
[14] J.A. Araújo, G.M.J. Almeida, J.L.A. Ferreira, C.R.M. da Silva, F.C. Castro, Early cracking orientation under high stress gradients: The fretting case, Int. J. Fatigue 100 (2017) 611–618.
[15] J. Vázquez, C. Navarro, J. Domínguez, On the estimation of fatigue life in notches differentiating the phases of crack initiation and propagation, Fatigue Fract. Eng. Mater Struct. 33 (2010) 22–36.
[16] C. Navarro, J. Vázquez, J. Domínguez, A general model to estimate life in notches and fretting fatigue, Eng. Fract. Mech. 78 (8) (2011) 1590–1601.
[17] J. Vázquez, C. Navarro, J. Domínguez, A model to predict fretting fatigue life including residual stresses, Theor. Appl. Fract. Mech. 73 (2014) 144–151.
[18] L. Bohórquez, J. Vázquez, C. Navarro, J. Domínguez, On the prediction of the crack initiation path in fretting fatigue, Theor. Appl. Fract. Mech. 99 (2019) 140–146.
[19] D. Erena, J. Vázquez, C. Navarro, Domínguez J. Carlos, A fretting fatigue model based on self-steered cracks, Theor. Appl. Fract. Mech. (2021), doi: https://doi.org/10.1016/j.tafmec.2021.103144.
[20] V. Martín, J. Vázquez, C. Navarro, J. Domínguez, Effect of shot peening residual stresses and surface roughness on fretting fatigue strength of Al 7075-T651, Tribol. Int. 142 (2020) 106004, https://doi.org/10.1016/j.triboint.2019.106004.
[21] V. Martín, J. Vázquez, C. Navarro, J. Domínguez, Fretting-fatigue analysis of shot-peened Al7075-T651 test specimens, Metals (Basel) 9 (5) (2019) 586, https://doi.org/10.3390/met9050586.
[22] A. Merati, G. Eastaugh, Determination of fatigue related discontinuity state of 7000 series of aerospace aluminum alloys, Eng. Fail Anal. 14 (4) (2007) 673–685.
[23] F. Czerwinski, Controlling the ignition and flammability of magnesium for aerospace applications, Corros. Sci. 86 (2014) 1–16.
[24] J. Vázquez, C. Navarro, J. Domínguez, Analysis of fretting fatigue initial crack path in Al7075-T651 using cylindrical contact, Tribol. Int. 108 (2017) 87–94.
[25] Alloy 7075 Plate and Sheet: Alcoa Mill Products: SPD-10-037, 2001.
[26] NIMS Fatigue Data Sheet No. 123: Data sheet on low-and high-cycle fatigue properties of A7075-T6 (Al-5.6Zn-2.5Mg-1.6Cu) Aluminium alloy. National Institute for Materials Sciences, Japan, 2017. ISSN 1347-3093.
[27] S. Muñoz, C. Navarro, J. Domínguez, Application of fracture mechanics to estimate fretting fatigue endurance curves, Eng. Fract. Mech. 74 (14) (2007) 2168–2186.
[28] Military Handbook - MIL-HDBK-5H: Metallic Materials and Elements for Aerospace Vehicle Structures, U.S. Department of Defense, ISBN 978-1-59124-543-8.
[29] C. Navarro, J. Vázquez, J. Domínguez, 3D vs. 2D fatigue crack initiation and propagation in notched plates, Int. J. Fatigue 58 (2014) 40–46.
[30] Kurath, P. (1978). Investigation into nonarbitrary fatigue crack size concept. Department of Theoretical and Applied Mechanics. College of Engineering. University of Illinois at Urbana-Champaign.
[31] J. Vázquez, C. Navarro, J. Domínguez, A new method for obtaining the stress field in plane contacts, Int J Solids Struct 49 (26) (2012) 3659–3665.
[32] D.F. Socie, Multiaxial fatigue damage models, ASME J. Eng. Mater. Technol. 109 (1987) 293–298.
[33] L. Susmel, P. Lazzarin, A bi-parametric Wöhler curve for high cycle multiaxial fatigue assessment, Fatigue Fract. Eng. Mater. Struct. 25 (1) (2002) 63–78.
[34] Y. Jiang, O. Hertel, M. Vormwald, An experimental evaluation of three critical plane multiaxial fatigue criteria, Int. J. Fatigue 29 (8) (2007) 1490–1502.
[35] A. Carpinteri, A. Spagnoli, S. Vantadori, Multiaxial fatigue life estimation in welded joints using the critical plane approach, Int. J. Fatigue 31 (1) (2009) 188–196.
[36] J.A. Araújo, A.P. Dantas, F.C. Castro, E.N. Mamiya, J.L.A. Ferreira, On the characterization of the critical plane with a simple and fast alternative measure of the shear stress amplitude in multiaxial fatigue, Int. J. Fatigue 33 (8) (2011) 1092–1100.
[37] J. Papuga, A survey on evaluating the fatigue limit under multiaxial loading, Int J Fatigue 33 (2) (2011) 153–165.
[38] J. Li, Z.-P. Zhang, Q. Sun, C.-W. Li, Multiaxial fatigue life prediction for various metallic materials based on the critical plane approach, Int. J. Fatigue 33 (2) (2011) 90–101.
[39] R. Brighenti, A. Carpinteri, S. Vantadori, Fatigue life assessment under a complex multiaxial load history: an approach based on damage mechanics, Fatigue Fract. Eng. Mater. Struct. 35 (2) (2012) 141–153.
[40] J.A. Araújo, A. Carpinteri, C. Ronchei, A. Spagnoli, S. Vantadori, An alternative definition of the shear stress amplitude based on the Maximum Rectangular Hull method and application to the C-S (Carpinteri-Spagnoli) criterion, Fatigue Fract. Eng. Mater. Struct. 37 (7) (2014) 764–771.
[41] F.C. Castro, J.A. Araújo, E.N. Mamiya, P.A. Pinheiro, Combined resolved shear stresses as an alternative to enclosing geometrical objects as a measure of shear stress amplitude in critical plane approaches, Int. J. Fatigue 66 (2014) 161–167.
[42] A. Carpinteri, A. Spagnoli, C. Ronchei, D. Scorza, S. Vantadori, Critical plane criterion for fatigue life calculation: time and frequency domain formulations, Procedia Eng. 101 (2015) 518–523.
[43] C.-C. Chu, Fatigue damage calculation using the critical plane approach, J. Eng. Mater. Technol. 117 (1995) 41–49.
[44] D.F. Socie, J. Morrow, W.C. Chen, A procedure for estimating the total fatigue life of notched and cracked members. Eng. Fract. Mech. 11(4) (1979) 851–859.
[45] Burden, Richard L.; Faires, J. Douglas (1985), «2.1 The Bisection Algorithm», Numerical Analysis, ISBN 0-87150-857-5 3rd ed. , PWS Publishers.
[46] T. Belytschko, T. Black, Elastic crack growth in finite elements with minimal remeshing, Int. J. Numer. Meth. Eng. 45 (1999) 601–620, https://doi.org/10.1002/(SICI)1097-0207(19990620)45:5<601::AID-NME598>3.0.CO;2-S.
[47] R. Hojjati-Talemi, M. Abdel Wahab, J. De Pauw, P. De Baets, Prediction of fretting fatigue crack initiation and propagation lifetime for cylindrical contact configuration, Tribol Int 76 (2014) 73–91, https://doi.org/10.1016/j.triboint.2014.02.017.
[48] E. Giner, M. Sabsabi, J.J. Ródenas, F.F. Javier, Direction of crack propagation in a complete contact fretting-fatigue problem, Int J Fatig 58 (2014) 172–180, https://doi.org/10.1016/j.ijfatigue.2013.03.001.
[49] J. Vázquez, C. Navarro, J. Domínguez, Two dimensional versus three dimensional modelling in fretting fatigue life prediction, J Strain Anal Eng Des 51 (2) (2016) 109–117.
[50] K. Tanaka, Fatigue crack propagation from a crack inclined to the cyclic tensile axis, Eng. Fract. Mech. 6 (3) (1974) 493–507.